




# Role of Advanced Magnetic Resonance Imaging in Differentiating among Glioma Subtypes and Predicting Tumor-Proliferative Behavior

Gunalan Ganesan<sup>1</sup>  Rajeswaran Rangasami<sup>1</sup> Anupama Chandrasekharan<sup>1</sup> Sahithi Marreddy<sup>1</sup>  
Rajoo Ramachandran<sup>1</sup>

<sup>1</sup> Department of Radiology, Sri Ramachandra Institute of Higher Education and Research, Chennai, Tamil Nadu, India

**Address for correspondence** Rajeswaran Rangasami, MBBS, MD, PhD, Sri Ramachandra Institute of Higher Education and Research, Chennai, Tamil Nadu 600116, India (e-mail: rajeswaranrangasami@gmail.com).

Asian J Neurosurg

## Abstract

**Objective** Gliomas are a devastating and heterogeneous group of primary brain tumors. Previously, the source of glioma was undetermined. Recent literature indicates that neural stem cells, or progenitors, are proposed to be the source of glioma. The prognosis of different types of gliomas differs due to their various biological tissue types. Besides the histological grade, the two useful immunohistochemistry markers that show the tumor's biological behavior are isocitrate dehydrogenase (IDH) labeling and the Ki-67 labeling index. We sought to determine the magnetic resonance imaging (MRI) characteristics associated with IDH mutational status and ascertain whether MRI combined with IDH mutational status, can better predict the clinical outcomes of gliomas.

**Materials and Methods** This period study was conducted in the Department of Radiology, Sri Ramachandra Institute of Higher Education and Research, Chennai, Tamil Nadu, India for 5 years (May 2016–May 2021). The study cohort included 30 patients diagnosed with gliomas who underwent preoperative MRI followed by surgical resection and histopathological examination. Preoperative MRI images were done to assess qualitative tumor characteristics such as location, margin of tumor, extent, cortical involvement, cystic component, mineralization or hemorrhage, and contrast enhancement.

**Discussion** Differences in MRI features between IDH-mutant (MT) and IDH-wild-type (WT) groups were analyzed using the chi-square test for categorical variables and the Mann–Whitney *U* test for continuous variables. Statistical analysis was conducted using SPSS software.

**Results** Among the 30 patients evaluated, 18 had IDH-WT and 12 had IDH-MT type gliomas. Male predominance (73.33%) was noted in our study. Brainstem location, indistinct borders (83.33%), less cortical involvement (72.22%), less cystic changes (88.89%), more area of necrotic component (44.44%), significantly increased choline/creatine (Cho/Cr) ratio, and choline/N-acetyl aspartate (Cho/NAA) ratio favors

## Keywords

- ▶ glioma
- ▶ IDH mutational status
- ▶ brain tumor
- ▶ astrocytoma
- ▶ glioblastoma

DOI <https://doi.org/10.1055/s-0044-1790508>.  
ISSN 2248-9614.

© 2024. Asian Congress of Neurological Surgeons. All rights reserved.

This is an open access article published by Thieme under the terms of the Creative Commons Attribution-NonDerivative-NonCommercial-License, permitting copying and reproduction so long as the original work is given appropriate credit. Contents may not be used for commercial purposes, or adapted, remixed, transformed or built upon. (<https://creativecommons.org/licenses/by-nc-nd/4.0/>)

Thieme Medical and Scientific Publishers Pvt. Ltd., A-12, 2nd Floor, Sector 2, Noida-201301 UP, India

IDH-WT tumors. Positive T2-fluid-attenuated inversion recovery mismatch sign is more frequently seen in IDH-MT (7/12; 58.33%) tumors than in IDH-WT (4/18; 22.22%) tumors. Whereas well-defined contours (66.67%), more cortical involvement (83.33%), more cystic changes (58.33%), and less area of necrotic component favor IDH-MT type tumors.

**Conclusion** MRI is a very promising and valuable tool for differentiating among glioma subtypes and predicting tumor-proliferative behavior in glioma cases. The combination of MRI characteristics with IDH mutation status enhances the predictive accuracy for clinical outcomes in glioma patients. This approach could potentially guide treatment planning and improve prognostic assessments.

## Introduction

Brain tumors are not a really common disease, but they are among the most fatal cancers. The causes of brain cancer are still largely unknown, the only environmental risk factors that could be identified so far are exposure to ionizing radiation.<sup>1</sup> Early detection of brain tumors is difficult because the tumors do not exhibit very specific clinical symptoms. In general, three different categories of symptoms for brain tumors can be distinguished.<sup>2</sup> First, increased cranial pressure can lead to headaches, vomiting, and altered states of consciousness. Second, cognitive and behavioral impairment, personality, or emotional changes can be attributed to brain dysfunction. And third, symptoms of irritation like absences, fatigue, or seizures can be observed. However, these symptoms are not specific to brain tumors alone. Gliomas account for 25.5% of primary brain and central nervous system (CNS) tumors and 80% of malignant tumors.<sup>3</sup> Gliomas develop from the supportive glial cells that consist of three major types: oligodendrocytes, astrocytes, and ependymal cells. Glial cells and neurons are the two major sorts of cells in the neural tissues. However, only glial cells can undergo cell division, and if the process of cell division is not carefully controlled and happens too fast, glioma forms and grows. The 2016 CNS World Health Organization (WHO) classification is based on a combined phenotypic and genotypic classification which led to the introduction of “integrated” diagnoses.<sup>4</sup> This updated classification of the gliomas is presented in the 2021 WHO Classification of Tumors of the CNS as illustrated in ►Fig. 1. The new classification of CNS tumors is increasingly defined by molecular markers.

In the 2016 WHO classification, isocitrate dehydrogenase (IDH)-mutant (MT) diffuse astrocytic tumors were assigned to three different tumor types (diffuse astrocytoma, anaplastic astrocytoma, and glioblastoma) depending on the histological parameters. In the current classification, the term glioblastoma is no longer applied to IDH-MT tumors; prior IDH-MT glioblastomas are now designated as astrocytoma, IDH-MT, and CNS WHO grade 4. New “families” of pediatric-type high-grade and low-grade diffuse gliomas include a variety of different tumor forms, some of which have distinct imaging properties. This new classification correlates with the patient’s treatment and survival. The histological types

have different clinical behavior; oligodendroglioma tumors are associated with longer survival when compared with astrocytoma.<sup>5</sup>

Low-grade gliomas (LGGs) are infiltrative tumors characterized by slow progression for several years, with a risk of anaplastic transformation into high-grade gliomas (HGGs). HGGs are malignant gliomas and the most lethal CNS tumors, characterized by aggressive infiltrative growth and a very poor prognosis despite intense therapeutic efforts. They have an annual incidence of approximately 4 to 5 per 100,000, and the approximate 5-year survival rate is 30%.<sup>3</sup> Glioma treatment depends on an accurate and early diagnosis and classification. The treatment of LGGs is either resection or regular monitoring, while the treatment of HGGs is mostly resection followed by radiotherapy and chemotherapy. Taking into account that the radiological growth rate of LGGs is approximately 4 mm/year,<sup>6</sup> early and accurate glioma grading is important for patient management and treatment planning. Histologic analysis is the gold-standard method to grade gliomas. However, this is an invasive technique, and involves sampling the glioma tissue which is susceptible to sampling error, furthermore, the continuous tumor growth might demand several biopsies for the same patient, additionally, not all of the glioma patients are operable. Magnetic resonance imaging (MRI) evolved to be the technique of choice for the characterization and classification of brain tumors. MRI is helpful for diagnostic evaluation of the anatomy, size, and vascular details of brain tumors.

## Materials and Methods

This period study was conducted in the Department of Radiology, Sri Ramachandra Institute of Higher Education and Research, Chennai, Tamil Nadu, India for 5 years (May 2016–May 2021). The images were acquired with GE Signa HDxt 1.5 Tesla or with Siemens Magnets Avanto 1.5 Tesla. Standard neurovascular coils in GE and head matrix coils in SIEMENS. The study was approved by the institution’s ethics committee. We analyzed 30 diagnosed glioma cases with preoperative MRI, histological grading, and immunohistochemistry.

Exclusion criteria include: postradiotherapy/chemotherapy/surgery cases, patients without histopathological follow-up, where image quality is not satisfactory, and patients

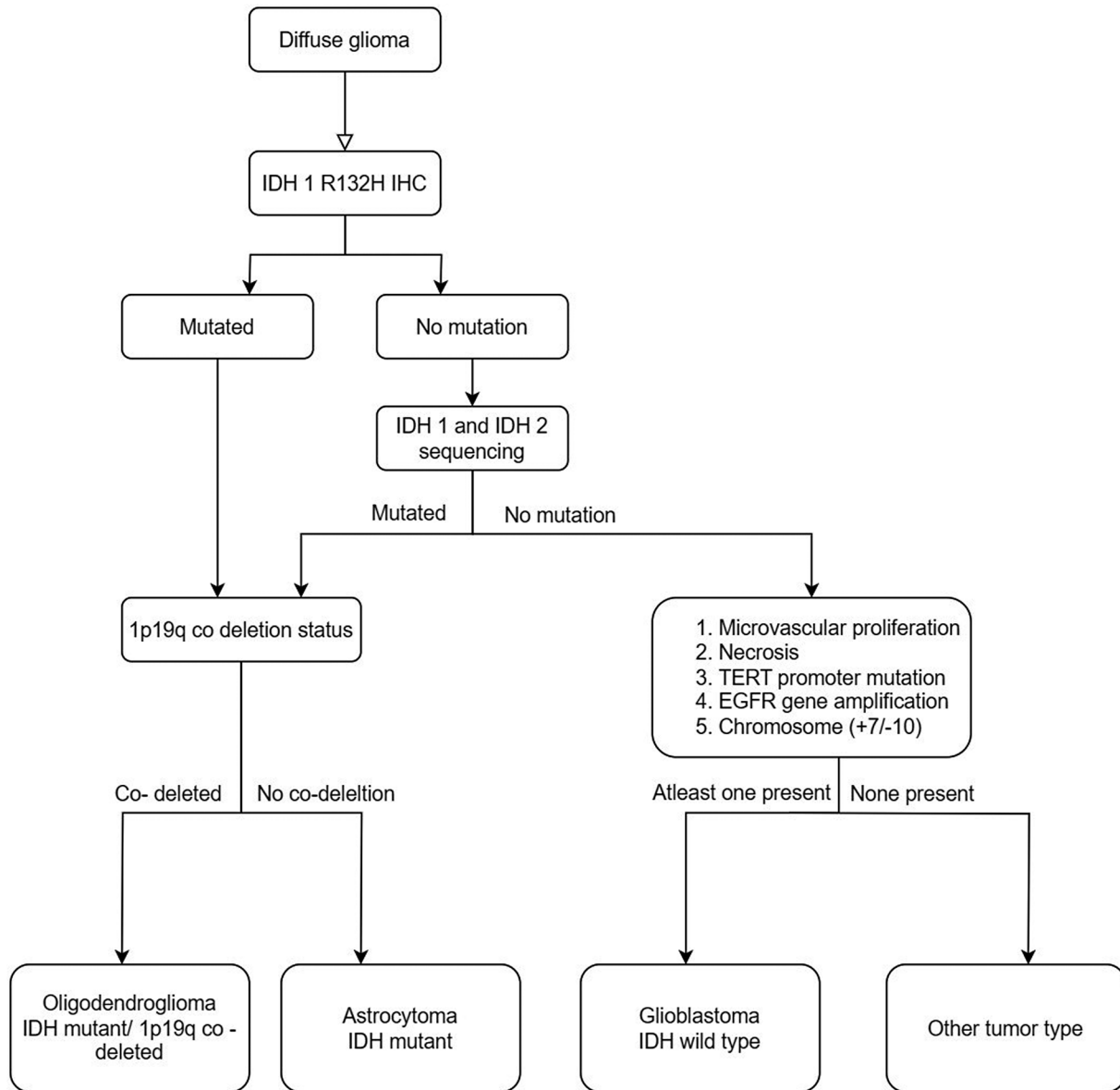


**Fig. 1** A simplified algorithm for classification of the diffuse gliomas based on histological and genetic features—2021 World Health Organization (WHO) Classification of Tumors of the central nervous system (CNS).

with contraindications to MRI. All the patients or their attendees who were referred for MRI brain were first explained about the MR procedure. A detailed clinical history was elicited, previous medical records were studied, and informed consent was obtained. The patient was then screened with a metal detector, positioned, and MR examination was performed. Conventional MRI of the brain was first performed with the following sequences: axial T1, axial T2, axial diffusion-weighted imaging, axial apparent diffusion coefficient, coronal T2 fluid-attenuated inversion recovery (FLAIR), axial gradient, and axial T1 fat-suppressed. Following the routine sequences, intravenous contrast (gadobenate dimeglumine 0.1 mmol/kg) was administered intravenously. Postcontrast sequences are then acquired as follows: axial and sagittal T1 and coronal three-dimensional spoiled gradient-recalled echo. Perfusion and MR spectroscopy (MRS) were also done.

The following MRI parameters were analyzed:

1. Location
2. Peritumoral edema
3. Contours
4. Multifocal/multicentric involvement
5. Cortical involvement
6. Cystic component
7. T2-FLAIR mismatch
8. Hemorrhagic component
9. Necrotic component
10. Contrast enhancement
11. MRS: choline-creatine ratio (Cho/Cr)
12. MRS: choline-N-acetyl aspartate (Cho/NAA) ratio

Stereotactic brain biopsy was done. IDH mutational status is obtained by performing immunohistochemistry and

sequencing on surgical biopsy specimens. Radiological data obtained from pre- and postcontrast sequences were correlated with the histopathological diagnosis and the immunohistochemistry results.

### Statistical Analysis

Both parametric (*t*-test) and nonparametric (Mann–Whitney's) tests of significance were done in the study groups using SPSS software. To assess diagnostic power, the areas under the curve (AUCs), binary logistic regression, and receiver operating characteristic analyses were plotted. The terms specificity,

accuracy, negative predictive value (NPV), positive predictive value (PPV), and sensitivity are used to describe diagnostic power. Statistical analysis was conducted using SPSS software. *p*-Values of < 0.05 were considered statistically significant.

### Results

The study comprised 30 patients with histologically proven diagnosis of glioma. This included 18 IDH-wild-type (WT) and 12 IDH-MT gliomas. Of these patients, 22 were male and 8 females, demonstrating a male predominance. **Table 1**

**Table 1** Characteristics of IDH mutant and wild-type brain tumors

| Characteristics               | IDH mutant tumors; N = 12 | IDH wild-type tumors; N = 18 | <i>p</i> -Value |
|-------------------------------|---------------------------|------------------------------|-----------------|
| Side                          |                           |                              |                 |
| Right                         | 2                         | 4                            | –               |
| Left                          | 7                         | 11                           |                 |
| Midline/Bilateral             | 3                         | 3                            |                 |
| Multifocal                    | 4 (33.33)                 | 6 (33.33)                    | 0.3667          |
| Multicentric                  | 0                         | 3 (16.67)                    |                 |
| Contours                      |                           |                              |                 |
| Well defined                  | 8 (66.67%)                | 3 (16.67%)                   | 0.0002          |
| Indistinct                    | 4 (33.33%)                | 15 (83.33%)                  |                 |
| Cortical involvement          |                           |                              |                 |
| Present                       | 10 (83.33%)               | 5 (27.78%)                   | 0.0028          |
| Absent                        | 2 (16.67%)                | 13 (72.22%)                  |                 |
| Peritumoral edema             |                           |                              |                 |
| Absent or slight              | 7 (58.33%)                | 4 (22.22%)                   | 0.0443          |
| Significant                   | 5 (41.67%)                | 14 (77.78%)                  |                 |
| Cystic changes                |                           |                              |                 |
| Present                       | 7 (58.33%)                | 2 (11.11%)                   | 0.0056          |
| Absent                        | 5 (41.67%)                | 16 (88.89%)                  |                 |
| Mineralization                |                           |                              |                 |
| Present                       | 5 (41.67%)                | 9 (50.00%)                   | 0.6540          |
| Absent                        | 7 (58.33%)                | 9 (50.00%)                   |                 |
| Contrast enhancement          |                           |                              |                 |
| > 25%                         | 4 (33.33%)                | 12 (66.67%)                  | 0.0729          |
| < 25%                         | 8 (66.67%)                | 6 (33.33%)                   |                 |
| Necrosis                      |                           |                              |                 |
| Present                       | 4 (33.33%)                | 12 (66.67%)                  | 0.0729          |
| Absent                        | 8 (66.67%)                | 6 (33.33%)                   |                 |
| Necrosis-tumor ratio > 22.5 % | 0                         | 8 (44.44%)                   | 0.0385          |
| Positive T2 FLAIR mismatch    | 7 (58.33%)                | 4 (22.22%)                   | 0.0443          |
| Negative T2–FLAIR Mismatch    | 5 (41.67%)                | 14 (77.78%)                  |                 |
| Spectroscopy (mean) Ch/NAA    | 2.49 ± 1.06               | 4.01 ± 2.47                  |                 |
| Spectroscopy (mean) Ch/Cr     | 1.98 ± 0.84               | 3.31 ± 1.87                  |                 |

Abbreviations: Ch/Cr, choline:creatinine; Ch/NAA, choline:N-acetyl aspartate; FLAIR, fluid-attenuated inversion recovery; IDH, isocitrate dehydrogenase.

summarizes the characteristics of IDH-MT and WT gliomas.

The age group of the patients ranged from 7 to 69 years, with a high incidence of 23.3% in the seventh decade. IDH-WT tumors were more common in the 7th decade (27.78%), followed by 6th decade (16.67%). The median age of IDH-WT tumors was 47 years, whereas that of IDH-MT was 45 years.

Among 16 IDH-MT tumors, 15 (93.75%) were in the lobar location and 1 (6.25%) was in central location. Also, 28 IDH-WT tumors (due to multicentric/multifocal distribution), were distributed as follows: 20 (71.42%) in lobar, 6 (21.43%) in central, and 2 (7.15%) in brainstem location (►Fig. 2). Among 12 IDH-MT tumors 2 were in the right side, 7 were in the left side, and 3 were in the midline/bilateral location. Also, among 18 IDH-WT tumors 4 were in the right side, 11 were in the left side, and 3 were in the midline/bilateral location. In IDH-MT tumors 8 (66.67%) tumors had well-defined borders compared with 4 (33.33%) tumors with indistinct borders. Among 18 IDH-WT tumors 3 (16.67%) tumors had well-defined borders compared with 15 (83.33%) tumors with indistinct borders. Cortical involvement was seen in 83.33% IDH-MT tumors versus 27.78% IDH-WT tumors. In our study, significant

peritumoral edema was seen in 41.67% IDH-MT tumors compared with 77.78% of IDH-WT tumors. Cystic changes were seen in 58.33% IDH-MT tumors compared with 11.11% of IDH-WT tumors. Mineralization or hemorrhage was seen in 41.67% IDH-MT tumors compared with 50.00% of IDH-WT tumors. The area and percentage of necrosis were higher in IDH-WT gliomas ( $24.50\% \pm 7.39\%$ ) than in IDH-MT gliomas ( $7.62\% \pm 2.16\%$ ), with a significant difference,  $p$ -value = 0.038 (►Fig. 3). Contrast enhancement was categorized into two patterns according to the volume of contrast enhancement: <25% versus >25%. IDH-WT tumors more frequently exhibited >25% volume enhancement (66.67%), whereas IDH-MT tumors showed <25% volume enhancement more commonly (66.67%) (►Fig. 4). Positive T2-FLAIR mismatch sign is more frequently seen in IDH-MT (7/12; 58.33%) tumors than in IDH-WT (4/18; 22.22%) tumors (►Fig. 5). In our study, the mean Cho/Cr ratio was  $3.31 \pm 1.87$  in the IDH-WT tumors group versus  $1.98 \pm 0.84$  in IDH-MT tumors. Also, mean Cho/NAA ratio was  $4.01 \pm 2.47$  in the IDH-WT tumors group versus  $2.49 \pm 1.06$  in IDH-MT tumors. Diagnostic performance parameters of each MRI characteristics in our study are listed in ►Table 2.

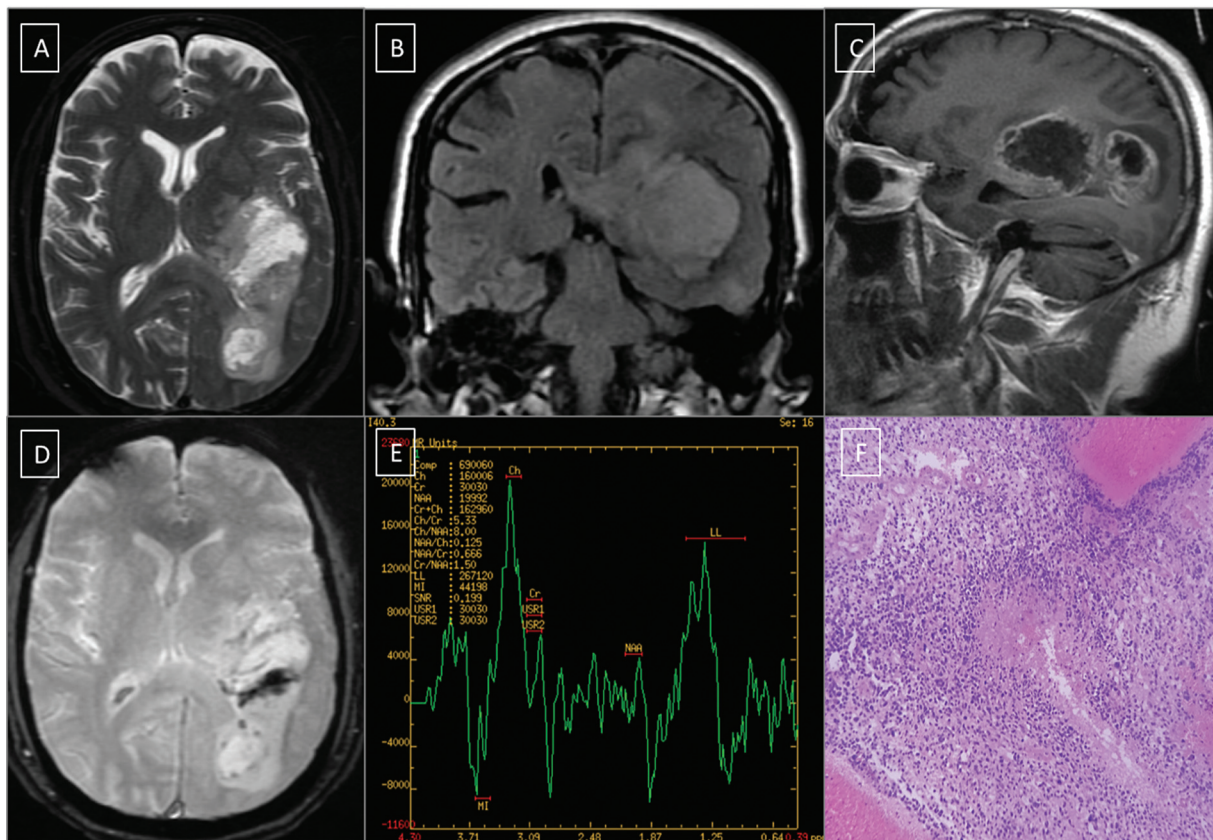


**Fig. 2** A 66-year-old male with history of fever and decreased response with left upper limb weakness. (A and B) Axial T2-weighted image and coronal T2 fluid-attenuated inversion recovery (FLAIR) showing a multifocal, ill-defined hyperintense signal intensity lesion involving the brainstem, left superior and middle cerebellar peduncles, bilateral hippocampus, subcortical white matter of bilateral anterior temporal lobe, and right frontal lobe with significant perilesional edema. (C and D) Postcontrast axial T1-weighted images—lesion in the right temporal lobe and the left hemispheres shows peripheral irregular contrast enhancement with few areas of necrosis. (E) Magnetic resonance (MR) spectroscopy values of the lesion—maximum choline:creatine and choline:N-acetyl aspartate (NAA) ratios are 3.38 and 1.85, respectively. (F) Histopathological analysis revealed World Health Organization (WHO) grade IV isocitrate dehydrogenase (IDH) wild-type glioblastoma multiforme.

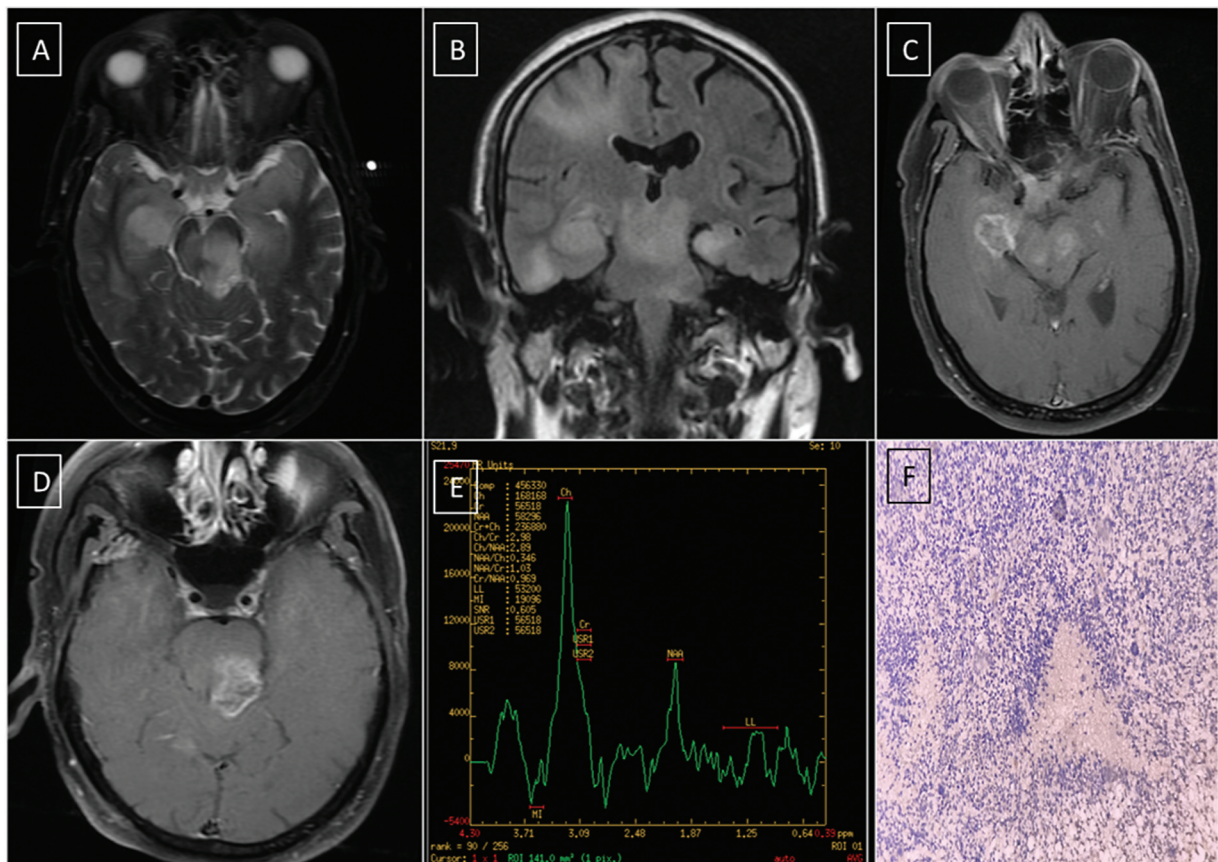


**Fig. 3** A 66-year-old male with complaints of right-sided weakness. (A) Axial T2-weighted image showing an ill-defined heterogeneous signal intensity lesion involving the left parietal, temporal, occipital periventricular white matter with significant perilesional edema. (B) Coronal T2 fluid-attenuated inversion recovery (FLAIR)—the lesion appears heterogeneous in signal intensity. (C) Postcontrast sagittal T1-weighted image—the lesion shows peripheral rim enhancement with areas of necrosis. (D) On gradient echo (GRE) sequence areas of mineralization or hemorrhage are seen within the lesion. (E) Magnetic resonance (MR) spectroscopy values of the lesion—maximum choline:creatine and choline:N-acetyl aspartate (NAA) ratios are 5.33 and 8, respectively. Elevated lipid lactate peaks are also seen consistent with necrosis. (F) Histopathological analysis revealed World Health Organization (WHO) grade IV isocitrate dehydrogenase (IDH) wild-type glioblastoma multiforme.

## Discussion

Our study included 30 patients, with a male preponderance (22 males, 8 females). The age group ranged from 7 to 69 years, with a peak incidence (23.3%) in the seventh decade. The median age of IDH-WT tumors was 47 years, while that of IDH-MT tumors was 45 years.

The primary site of tumor involvement was categorized as lobar (cerebrum and cerebellum), central (optic chiasma, ventricle, basal ganglia, and thalamus), or brainstem. In our study, IDH-MT tumors were distributed as follows based on lobar anatomy: eight frontal, three temporal, and one frontotemporal with hippocampus involvement. Frontal tumors were more frequently IDH-MT tumors (8/12) while all brainstem tumors are IDH-WT tumors. In our study, 93.75% of IDH-MT types of tumors are seen involving the lobar location and 71.42% of IDH-WT tumors are seen in lobar locations. Also, 21.43% IDH-WT tumors are seen to involve central location, whereas only 6.25% IDH-MT tumors are seen to involve central location. Our study correlates with the study conducted by Villanueva-Meyer et al, where all brainstem tumors were IDH-WT tumors.<sup>7</sup> Also, they have found that there is higher prevalence of IDH-MT type tumors

involving lobar location compared with their wild counterparts, however, that did not meet statistical significance. Multifocal tumors affect multiple regions connected by direct dissemination pathways like subependymal or white matter tracts, while multicentric tumors affect multiple regions without discernible dissemination routes. In our study, there was a trend toward a higher frequency of multifocal/multicentric distribution in IDH-WT tumors (50.0%) that did not meet statistical significance ( $p = 0.366$ ). In studies conducted by Park et al and Villanueva-Meyer et al, they have found that IDH-WT tumors have higher frequency of multifocal/multicentric distribution.<sup>7,8</sup>

In our study, IDH-MT tumors have better defined contours than IDH-WT tumors. Note that 83.33% of IDH-WT tumors have indistinct borders, whereas only 33.33% of IDH-MT tumors have indistinct borders ( $p$ -value = 0.00024). Our study correlates with Ding et al, wherein they have stated that IDH-WT tumors (66.6%) have higher frequency of indistinct borders compared with their IDH-MT (39.1%) counterparts.<sup>9</sup> Also, in a study conducted by Metellus et al, they found that 100% of IDH-WT tumors in their cohort had indistinct borders in contrast to only 45% of IDH-MT tumors.<sup>10</sup> IDHMT tumors (83.33%) have a higher proportion

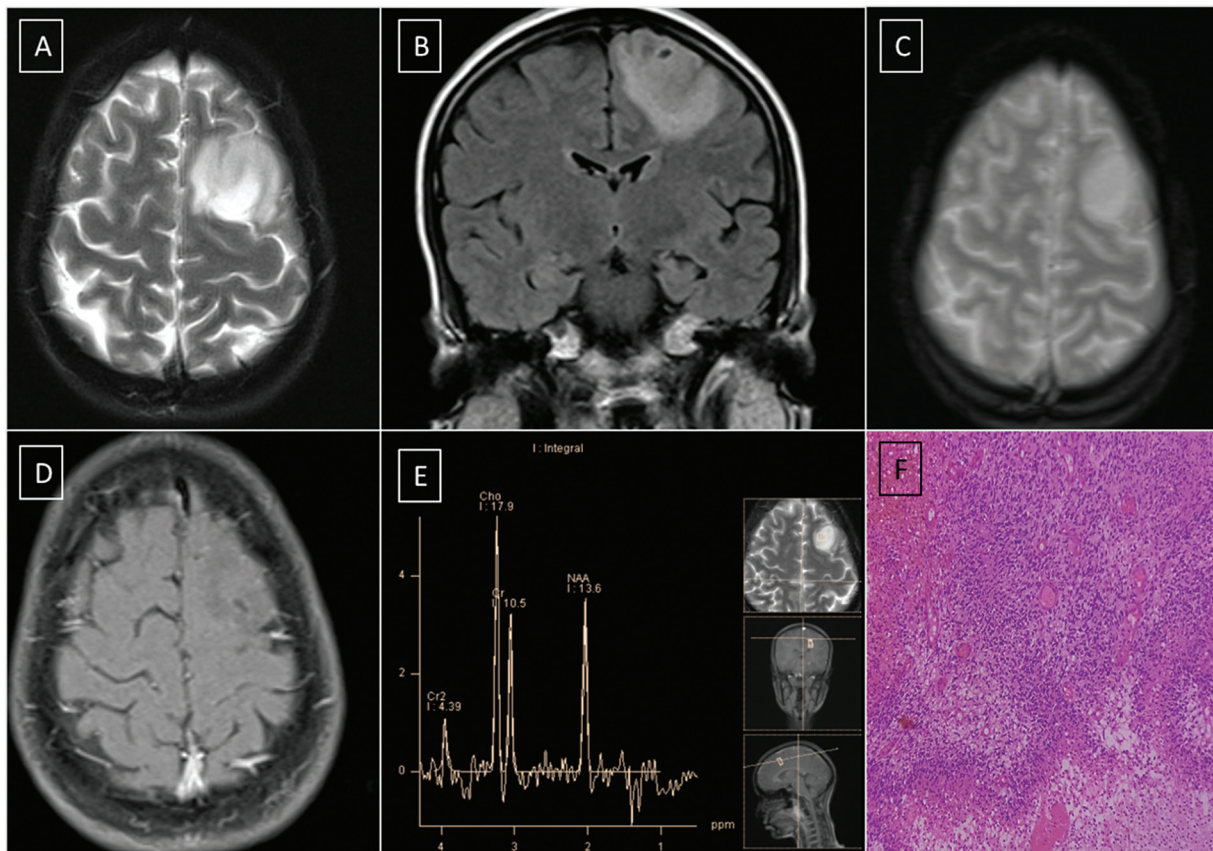


**Fig. 4** A 29-year-old female with complaints of seizures. (A and B) Axial T2-weighted image and coronal T2 fluid-attenuated inversion recovery (FLAIR) showing relatively well-defined hyperintense signal intensity lesion in the left frontal lobe involving superior frontal gyrus. (C) On gradient echo (GRE)—no evidence of blooming noted. (D) Postcontrast coronal T1-weighted image—the lesion shows no significant contrast enhancement. (E) Magnetic resonance (MR) spectroscopy values of the lesion—maximum choline:creatine and choline:N-acetyl aspartate (NAA) ratios are 1.7 and 1.31, respectively. (F) Histopathological analysis revealed World Health Organization (WHO) grade II isocitrate dehydrogenase (IDH) mutant type diffuse astrocytoma.

of cortical involvement than their wilder counterparts (27.78%),  $p$ -value = 0.0028. Our study correlates with Ding et al, wherein they have stated that IDH-MT type tumors (73.9%) more commonly involve the cortex than IDH-WT (25%).<sup>9</sup> We found that there is increased incidence (58.33%) of cystic changes in the IDH-MT tumors. Whereas only 11.15% of IDH-WT tumors have cystic changes,  $p$ -value = 0.005. In studies conducted by Villanueva-Meyer et al and Ding et al, they found a trend toward a higher frequency of cystic changes in IDH-MT type tumors that did not meet statistical significance.<sup>7,9</sup>

Peritumoral edema was determined based on its non-enhancement on contrast-enhanced T1-weighted image and higher signal on T2 FLAIR as an indicator of tumor cell infiltration. In our study, significant peritumoral edema is more frequently encountered in IDH-WT tumors (77.78%) as compared with IDH-MT tumors (41.67%). Preference of peritumoral edema in IDH-WT gliomas corresponds with their higher invasiveness.<sup>11</sup> Our study correlates with the study conducted by Ding et al, wherein they stated that higher frequency of IDH-WT tumors (58.4%) have infiltrative peritumoral edema compared with their mutant (32.6%) counterparts.<sup>9</sup> Nodular or ring-like enhancement is associated with blood–brain barrier breakdown and angiogenesis.

High permeability of tumor vessels leads to the leakage of gadolinium contrast to surrounding tumor tissue, which attributes to enhancement in MRI. In our study, contrast enhancement is categorized into two patterns according to the volume of contrast enhancement: < 25% versus > 25%. We found > 25% volume of contrast enhancement is more frequently encountered in IDH-WT tumors (66.67%) as compared with IDH-MT tumors (33.33%). However, that did not meet statistical significance,  $p$ -value = 0.0729. In a study conducted by Ding et al, they stated that IDH mutated glioblastomas often have a greater proportion of noncontrast enhancing tumors compared with IDH-WT glioblastomas.<sup>9</sup>

The central nonenhancing portion of the tumor represents the necrotic component. Necrosis area and necrosis percentage were higher in gliomas of IDH-WT ( $24.50\% \pm 7.39\%$ ) than in the IDH-MT counterpart ( $7.62\% \pm 2.16\%$ ),  $p$ -value = 0.038. Yamashita et al suggest the cutoff value of 22.5% of necrosis percentage (sensitivity, 72.7%; specificity, 81.8%; and accuracy, 74.2).<sup>12</sup> Our study correlates with Yamashita et al and Arevalo et al, where they have stated that IDH-WT tumors have higher necrosis percentage than IDH-MT tumors.<sup>12,13</sup> T2-FLAIR mismatch sign, which is defined as the presence of hyperintense signals on a T2-weighted image and a relatively hypointense signal on FLAIR except for a hyperintense peripheral rim, has

**Table 2** Diagnostic performance parameters of each MRI characteristic

|                      | Sensitivity | Specificity | PPV    | NPV    | Accuracy | LR+ | DOR  |
|----------------------|-------------|-------------|--------|--------|----------|-----|------|
| Contours             | 83.33%      | 66.67%      | 78.95% | 72.73% | 76.67%   | 2.5 | 9.9  |
| Cortical involvement | 72.22%      | 58.33%      | 72.22% | 58.33% | 66.67%   | 1.7 | 3.6  |
| Peritumoral edema    | 77.78%      | 58.33%      | 73.68% | 63.64% | 70.00%   | 1.9 | 4.9  |
| Cystic changes       | 88.89%      | 58.33%      | 76.19% | 77.78% | 76.67%   | 2.1 | 11.1 |
| Mineralization       | 50.00%      | 58.33%      | 64.29% | 43.75% | 53.33%   | 1.2 | 1.4  |

Abbreviations: DOR, diagnostic odds ratio; LR +, positive likelihood ratio; MRI, magnetic resonance imaging; NPV, negative predictive value; PPV, positive predictive value.

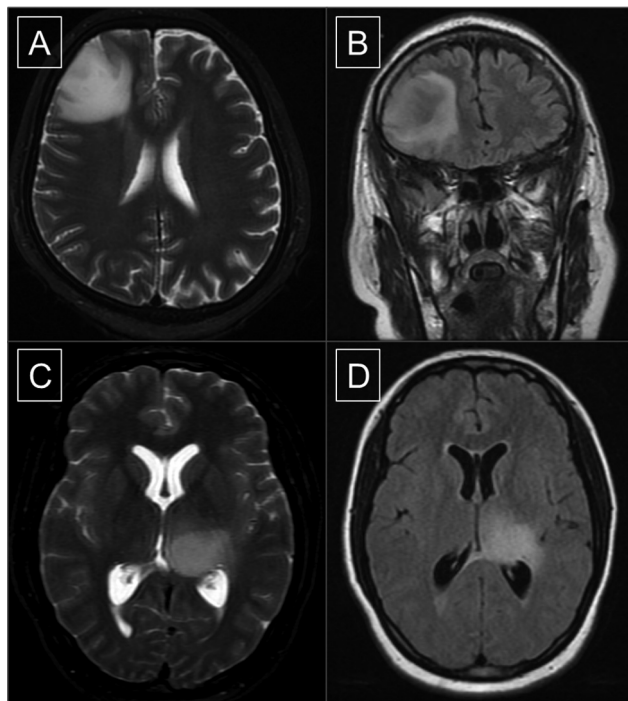


**Fig. 5** T2/fluid-attenuated inversion recovery (FLAIR) mismatch sign. (A and B) Axial T2-weighted image showing relatively well-defined hyperintense signal intensity lesion in the right frontal lobe, which shows hypointense signal on coronal T2 FLAIR indicating positive T2/FLAIR mismatch sign in favor of isocitrate dehydrogenase (IDH) mutant type glioma. (C and D) Axial T2-weighted and FLAIR images shows an ill-defined hyperintense signal intensity lesion involving the left thalamus with significant perilesional edema indicating negative T2/FLAIR mismatch sign in favor of IDH wild-type glioma.

been suggested and validated as a highly specific imaging marker of IDH-MT astrocytoma.<sup>14</sup> In our study, the positive T2-FLAIR mismatch sign is more frequently seen in IDH-MT (58.33%) tumors than IDH-WT (22.22%) tumors. Our study correlates with Deguchi et al, where they stated positive T2-FLAIR mismatch sign as a marker of IDH-MT astrocytoma with PPV of 83% and NPV of 77%.<sup>14</sup>

MRS provides details about the metabolic composition of tissue; three essential parameters have been quantitatively assessed to indicate physiology and pathology status of the tissue including: choline signifying membrane turnover and proliferation, creatinine which represents energy homeostasis, and NAA representing intact glioneuronal structures. The high Cho/Cr ratio is thought to be a malignant feature

and useful in predicting the histological grade of gliomas, which also indicates the higher invasiveness of gliomas.<sup>15</sup> In our study, we found that Cho/Cr ratio was significantly higher for IDH-WT tumors as compared with IDH-MT tumors, with an optimal AUC cutoff value of 1.88 and a sensitivity of nearly 83.3%. This suggested that the Cho/Cr ratio could represent an appealing imaging indicator for noninvasive assessment of the IDH status of gliomas. Study conducted by Narayana et al focused on Cho/Cr ratios and proposed a newer method for delineating target volume in gliomas.<sup>16</sup> Concretely, grade 0 was defined as Cho/Cr ratio < 1, indicating no tumor activity; grade 1 as Cho/Cr ratio of 1 to 2, meaning some tumor activity, correlating with microscopic disease; grade 2 represented as Cho/Cr ratio of 2 to 3, correlating with more aggressive anaplastic tumors; and grade 3 for Cho/Cr ratio 3 referring the most aggressive area, signifying the gross target volume.<sup>17</sup> Our results were consistent with this grading: mean Cho/Cr ratio was  $3.31 \pm 1.87$  in the IDH-WT tumors group corresponding to grade 3, indicating more aggressive feature, while mean Cho/Cr ratio in IDH-MT tumors was  $1.98 \pm 0.84$ , signifying less invasiveness. Also, in the study conducted by Ding et al, they found that the Cho/Cr ratio was significantly lower for IDH-MT type gliomas in comparison with the IDH-WT tumors group.<sup>18</sup> Mean Cho/Cr ratio in their study was 3.235 in the IDH-WT tumors group corresponding grade 3, indicating a more aggressive feature, while mean Cho/Cr ratio in IDH-MT tumors was 2.163. In our study, we also found that the mean Cho/NAA ratio was significantly higher for IDH-WT ( $4.01 \pm 2.47$ ) gliomas in comparison with the IDH-MT ( $2.49 \pm 1.06$ ) group.

## Conclusion

MRI is a powerful tool for differentiating among glioma subtypes and predicting IDH mutational status. Ongoing technological advancements in neuroimaging promise to enhance noninvasive tumor characterization, improving diagnostic accuracy and patient outcomes.

### Authors' Contributions

G.G. did the major write up of this review article. Majority of the cases in this review article were diagnosed and followed up by G.G. and R.R. The work was carried under the guidance of R.R. and he provided us the insight and knowledge to diagnose indeterminate lesions with



imaging alone. All the authors read the rough draft and provided valuable suggestions for the final draft. G.G. reviewed this article for corrections and final draft.

#### Funding

None.

#### Conflict of Interest

None declared.

#### Acknowledgments

The authors would like to thank their great and beloved teachers, closest friends, and mentors for their aid in completing this article.

#### References

- 1 Singh MS, Michael M. Role of xenobiotic metabolic enzymes in cancer epidemiology. *Methods Mol Biol* 2009;472:243–264
- 2 Buckner JC, Brown PD, O'Neill BP, Meyer FB, Wetmore CJ, Uhm JH. Central nervous system tumors. *Mayo Clin Proc* 2007;82(10):1271–1286
- 3 Wen PY, Schiff D, Cloughesy TF, et al. A phase II study evaluating the efficacy and safety of AMG 102 (rilotumumab) in patients with recurrent glioblastoma. *Neuro-oncol* 2011;13(04):437–446
- 4 Louis DN, Perry A, Reifenberger G, et al. The 2016 World Health Organization Classification of Tumors of the Central Nervous System: a summary. *Acta Neuropathol* 2016;131(06):803–820
- 5 Ohgaki H, Kleihues P. Population-based studies on incidence, survival rates, and genetic alterations in astrocytic and oligodendroglial gliomas. *J Neuropathol Exp Neurol* 2005;64(06):479–489
- 6 Mandonnet E, Delattre J-Y, Tanguy M-L, et al. Continuous growth of mean tumor diameter in a subset of grade II gliomas. *Ann Neurol* 2003;53(04):524–528
- 7 Villanueva-Meyer JE, Wood MD, Choi BS, et al. MRI features and IDH mutational status of grade II diffuse gliomas: impact on diagnosis and prognosis. *AJR Am J Roentgenol* 2018;210(03):621–628
- 8 Park YW, Han K, Ahn SS, et al. Prediction of IDH1-mutation and 1p/19q-codeletion status using preoperative MR imaging phenotypes in lower grade gliomas. *AJNR Am J Neuroradiol* 2018;39(01):37–42
- 9 Ding H, Huang Y, Li Z, et al. Prediction of IDH status through MRI features and enlightened reflection on the delineation of target volume in low-grade gliomas. *Technol Cancer Res Treat* 2019;18:1533033819877167
- 10 Metellus P, Coulibaly B, Colin C, et al. Absence of IDH mutation identifies a novel radiologic and molecular subtype of WHO grade II gliomas with dismal prognosis. *Acta Neuropathol* 2010;120(06):719–729
- 11 Stummer W. Mechanisms of tumor-related brain edema. *Neurosurg Focus* 2007;22(05):E8
- 12 Yamashita K, Hiwatashi A, Togao O, et al. MR imaging-based analysis of glioblastoma multiforme: estimation of IDH1 mutation status. *AJNR Am J Neuroradiol* 2016;37(01):58–65
- 13 Arevalo OJ, Valenzuela R, Esquenazi Y, et al. The 2016 World Health Organization Classification of Tumors of the Central Nervous System: a practical approach for gliomas, part 2. Isocitrate dehydrogenase status—imaging correlation. *Neurographics* 2017;7(05):344–349
- 14 Deguchi S, Oishi T, Mitsuya K, et al. Clinicopathological analysis of T2-FLAIR mismatch sign in lower-grade gliomas. *Sci Rep* 2020;10(01):10113–10125
- 15 Xu YJ, Cui Y, Li HX, et al. Noninvasive evaluation of radiation-enhanced glioma cells invasiveness by ultra-high-field (1)H-MRS in vitro. *Magn Reson Imaging* 2016;34(08):1121–1127
- 16 Li X, Jin H, Lu Y, Oh J, Chang S, Nelson SJ. Identification of MRI and 1H MRSI parameters that may predict survival for patients with malignant gliomas. *NMR Biomed* 2004;17(01):10–20
- 17 Narayana A, Chang J, Thakur S, et al. Use of MR spectroscopy and functional imaging in the treatment planning of gliomas. *Br J Radiol* 2007;80(953):347–354
- 18 Chang J, Thakur S, Perera G, et al. Image-fusion of MR spectroscopic images for treatment planning of gliomas. *Med Phys* 2006;33(01):32–40